Microwave Synthesis and Optical Properties of Uniform Nanorods and Nanoplates of Rare Earth Oxides

ARTICLE *in* THE JOURNAL OF PHYSICAL CHEMISTRY C · JANUARY 2007

Impact Factor: 4.77 · DOI: 10.1021/jp0670283

3 AUTHORS, INCLUDING:

Asit baran Panda
Central Salt and Marine Chemicals Research …
91 PUBLICATIONS **1,571** CITATIONS
SEE PROFILE

M. Samy El-Shall
Virginia Commonwealth University
273 PUBLICATIONS **4,633** CITATIONS
SEE PROFILE

THE JOURNAL OF PHYSICAL CHEMISTRY C LETTERS

Published on Web 01/12/2007

Microwave Synthesis and Optical Properties of Uniform Nanorods and Nanoplates of Rare Earth Oxides

Asit B. Panda, Garry Glaspell, and M. Samy El-Shall*

Department of Chemistry, Virginia Commonwealth University, Richmond, Virginia 23284-2006

Received: October 26, 2006; In Final Form: December 8, 2006

We report on the rapid production, characterization, and spectral properties of uniform nanorods, nanowires, and nanoplates of rare earth oxides (M_2O_3, M = Pr, Nd, Sm, Eu, Gd, Tb, Dy). The method developed, based on microwave irradiation (MWI), allows the control of the size and shape of the rare earth oxide nanostructures by varying the MWI reaction time and the relative concentrations of the organic surfactants. The uniformity of the rods and of the wires is demonstrated in their spontaneous assembly into highly ordered 2D supercrystals. The MWI method provides a unique opportunity for the large-scale synthesis of rare earth nanostructures without suffering thermal gradient effects.

The dependence of the properties of nanoscale materials on both the size and shape of the nanocrystal is a phenomenon of both fundamental scientific interest and many practical and technological applications.[1] In order to advance the basic understanding of the principles that determine the shape and to provide tailored building blocks for nanodevices, a variety of methods have been developed to control the shape, dimensionality, and assembly of nanostructures.[1−3] The shape control and assembly of nanostructures into organized patterns provide valuable routes to the design of functional materials and to a variety of device applications.[1−3] Rare earth oxides with one-dimensional structures represent a particularly interesting class of materials because of their unique electronic, optical, magnetic, and catalytic properties arising from the confinement of the 4f electrons.[4−7] These properties are critical for many interesting applications involving, for example, optical displays, optical communication, UV shielding, medical diagnostics, and efficient catalysis for the oxidation of heavy oils, jet fuels, and coal gasification.[8−12] Despite intensive experimental efforts, a simple, versatile, and general method for synthesizing shape-controlled rare earth oxide nanostructures has been lacking.[13−20] Several methods have been developed for the synthesis of rare-earth fluorides, hydroxides, and orthophosphate nanostructures.[21−24] The reported methods require high temperatures (300−330 °C) and relatively long reaction times under inert atmospheres.[13−20] Here we report the development of a rapid, simple, and versatile microwave irradiation (MWI) methodology for the synthesis of organically passivated uniform, single crystalline rare earth oxide (M_2O_3, M = Pr, Nd, Sm, Eu, Gd, Tb, Dy) nanorods (∼1.2 × 4−5 nm) and square nanoplates (6 × 6 nm). The as-synthesized rods form two-dimensional (2D) superlattice structures via a self-organization process.

MWI methods, in addition to providing simple and fast routes to nanomaterials, are unique in their potential for large-scale synthesis without suffering thermal gradient effects.[22,25−30] The rapid transfer of energy directly to the reactants (faster than they are able to relax) causes an instantaneous internal temperature rise. This allows the rapid decomposition of the nanocrystal precursors, thus creating highly supersaturated solutions where nucleation and growth can take place to produce the desired nanocrystalline products. Selective adsorption of organic surfactants can effectively inhibit the growth of the nanocrystal in all but the favorable crystallographic plane where the growth is significantly enhanced, thus resulting in a 1D structure. Because in MWI it is possible to quench the reaction very early on (∼10 s), this provides the opportunity to control the nanostructures from small spherical nuclei to short rods to extended assemblies of nanowires by varying the MWI reaction time and the concentration of the organic surfactants. In spite of these significant advantages, MWI has not been fully explored and only a few reports have been published on the synthesis of 1D nanomaterials.[27,28,30] Here we establish the MWI approach as a general procedure for the synthesis of nanorods and nanoplates of the rare earth oxides.

In a typical reaction, 5×10^{-4} mol of metal acetate or acetylacetonate (Aldrich) was dissolved in 6.8×10^{-3} mol of oleic acid (Aldrich) and 1.1×10^{-2} mol of oleylamine (Aldrich) at 110 °C in an oil bath under vigorous stirring for 5 min. The resulting solution was placed in a conventional microwave oven with the power set to 70% of 650 W and operated in 3 min cycles (on for 2.5 min, off and stirring for 30 s). After microwaving for the desired time, the synthesized rods were washed with ethanol, centrifuged, and re-dispersed in hydrophobic solvents such as toluene or dichloromethane.

To compare the effect of microwave irradiation with direct heating, we performed control experiments under identical reaction conditions to the microwave experiments but using conventional thermal heating. The resulting nanorods were significantly less uniform than those obtained under the microwave irradiation. This indicates that microwave irradiation results in better control of the morphology probably because of the significant shortening of the reaction time.

* Corresponding author. E-mail: selshall@hsc.vcu.edu.

10.1021/jp0670283 CCC: $37.00

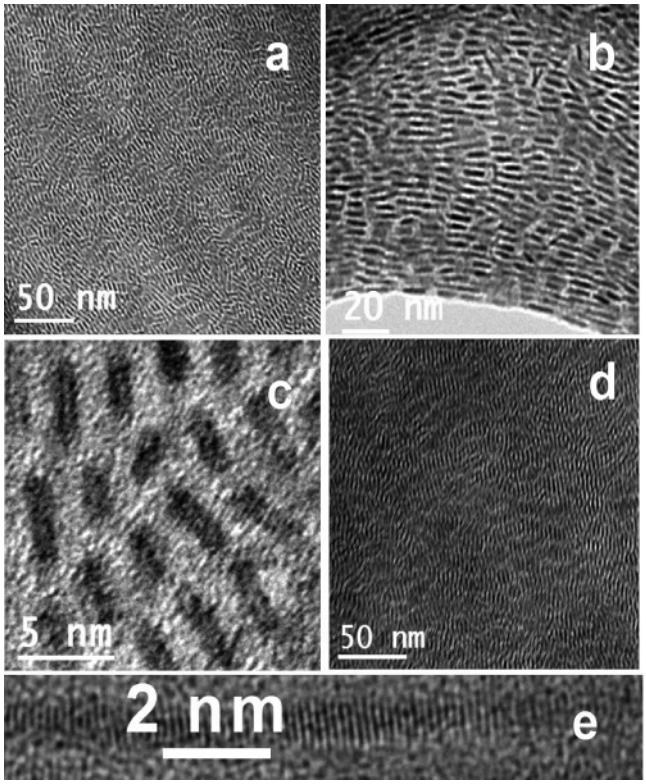

Figure 1. TEM images of (a and b) Sm_2O_3 nanorods forming 2D supercrystalline assembly, (c) HRTEM of Nd_2O_3 nanorods, (d) Gd_2O_3 nanowires, and (e) HRTEM of a Gd_2O_3 nanowire.

Figure 1 displays TEM images of the as-synthesized Sm_2O_3, Nd_2O_3, and Gd_2O_3 nanorods and nanowires. The nanorods with an average diameter of 1.2 nm and an average length of 4−5 nm are self-assembled into large regions of highly ordered, crystalline 2D superstructures as shown in Figure 1a and b.

For all of the rare earth oxides studied, 5−7 min of microwaving produced very small spherical or little elongated particles as shown in Figure 2, in 10 min rods were formed, and in 15 min mixtures of short and long connected rods (1.2 × 20−100 nm) were obtained. At longer microwaving times, the nanorods connected together to form long wires probably via an oriented attachment mechanism.[31] The wires have the same narrow widths as the short rods (1.2 nm) and lengths that vary from 20 to 100 nm as shown in the TEM images displayed in Figure 2 (bottom). The relative amount of rods and square plates can be controlled by the microwaving time and the relative concentrations of the metal precursor, the oleic acid, and the oleylamine.

To verify the circular rod shape as opposed to disks standing on the surface of the TEM grid,[18,19] grid tilting experiments were performed.[32] By tilting the grid (+20 and −20°) along the short axis of the rods, no variations in the observed thickness of the rods were found as shown in Figure 3.

High-resolution TEM (HRTEM) was used to further investigate the crystallinity and crystal structure of the synthesized nanostructures. Distinct lattice planes in the HRTEM image further suggest that all of the nanostructures are single crystals. The HRTEM image of the individual rods and wires (Figure 1e) shows well-resolved lattice planes perpendicular to the long axis with an interplanar distance corresponding to the *d* spacing of the (400) plane of the cubic *Ia*3 space group. This implies that rods are strictly growing through the [100] direction and confined along the [010] and [001] directions.

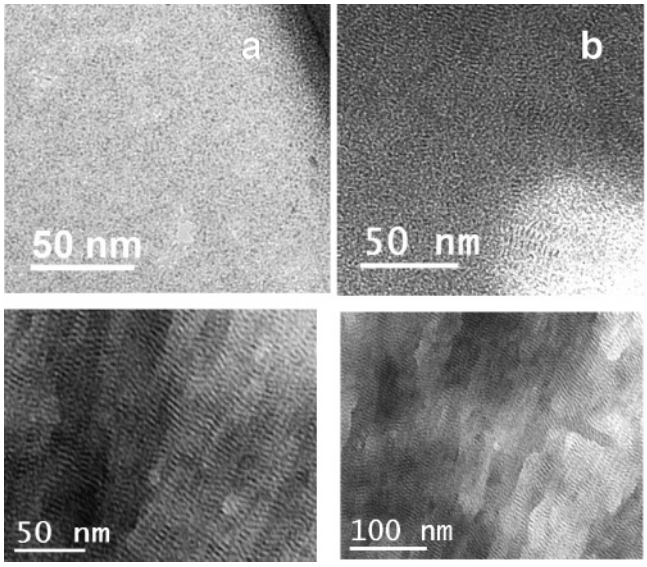

Figure 2. TEM images of (a) intermediate more spherical and (b) elongated nuclei of Sm_2O_3 following microwave irradiation for 5 and 7 min, respectively, of the reaction mixture containing 4.9×10^{-4} mol of samarium acetate, 6.6×10^{-3} mol of oleic acid, and 1.1×10^{-2} mol of oleylamine. The bottom images show Pr_2O_3 nanowires produced following microwave irradiation for 15 min of the reaction mixture containing 5×10^{-4} mol of praseodymium acetate, 6.6×10^{-3} mol of oleic acid, and 1.1×10^{-2} mol of oleylamine.

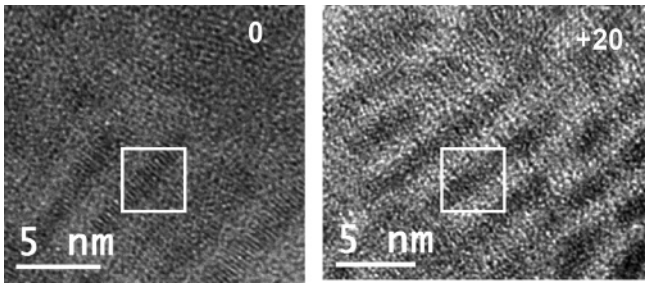

Figure 3. TEM images of tilting experiments of the Eu_2O_3 nanowires. (Left) no tilting and (right) +20° tilting of the TEM grid.

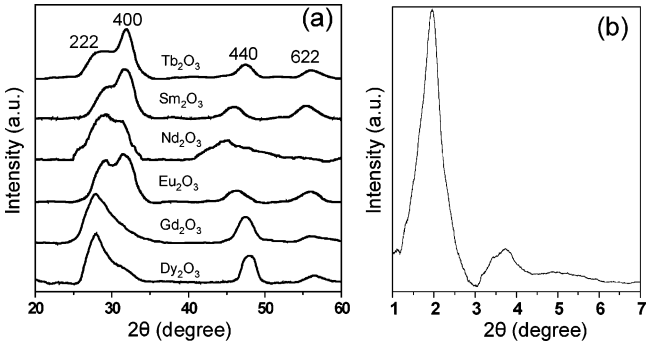

Figure 4. (a) XRD patterns of the synthesized rare earth oxide nanorods. (b) Small-angle XRD of the assembly of Eu_2O_3 nanorods.

The orientation of the lattice planes found in the TEM images is consistent with the XRD patterns shown in Figure 4a, which exhibit an intensity enhancement of the (400) peak in the patterns for the Tb_2O_3, Sm_2O_3, Nd_2O_3, and Eu_2O_3 nanorods compared to the standard patterns for the corresponding bulk rare earth oxide. This is in contrast to the XRD patterns of the Tb_2O_3 and Eu_2O_3 nanoplates prepared by the thermolysis of the corresponding benzoylacetonate complexes in oleic acid/oleylamine solvents at 310 °C where the diffraction intensity from the (400) plane was significantly diminished and no sharp

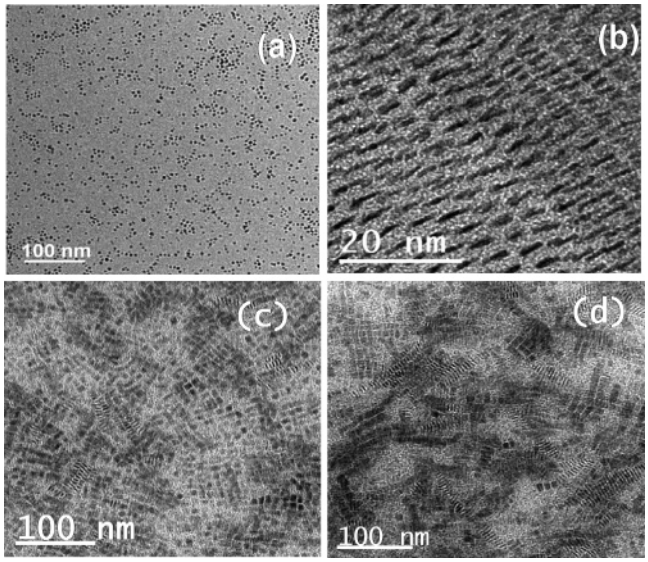

Figure 5. (a) TEM image of spherical Eu_2O_3 nanoparticles synthesized using a mole ratio of metal acetate/oleic acid/oleylamine corresponding to 1:17:17. (b) Eu_2O_3 nanorods synthesized using a mole ratio of oleylamine/oleic acid corresponding to 1.5. (c) Sm_2O_3 and (d) Eu_2O_3 mixtures of square nanoplates and nanorods synthesized using a higher mole ratio of oleylamine/oleic acid (3:1).

peak could be identified.[19] Figure 4b displays the small-angle XRD spectrum, which confirms the assembly of the rods into ordered 2D supercrystals.

The growth mechanism for the 1D rare earth nanostructures can be attributed to kinetic growth, which determines the final morphology of the nanocrystals rather than thermodynamic growth. In this case, competitive adsorption of oleic acid and oleylamine effectively can inhibit the growth of the nanocrystal in all but the favorable crystallographic plane where the growth is significantly enhanced, thus resulting in a 1D structure.[32,33] The crystal plane with a higher surface energy is expected to have a faster growth rate. To verify this mechanism, we varied the relative concentrations of oleic acid and oleylamine in the MWI syntheses. When the mole ratio of the metal precursor/oleic acid/oleylamine was 1:17:17, spherical particles were formed as shown in Figure 5a for the case of Eu_2O_3 nanocrystals. This is consistent with the stronger binding capability of oleic acid relative to oleylamine,[20] and therefore it binds strongly with the atoms of all of the planes and the thermodynamic limit (3D) is approached in the presence of excess oleic acid. The nanorods are formed when the mole ratio of oleylamine to oleic acid is about 1.5 as shown in Figure 5b for Eu_2O_3 nanocrystals. However, when oleylamine was present in much excess, square nanoplates were formed as shown for Sm_2O_3 and Eu_2O_3 in Figure 5c and d, respectively. From repeated sets of experiments under the same microwaving time, we found that the nanorods and the square nanoplates were predominantly formed when the mole ratios of the metal acetate/oleic acid/oleylamine were 1:14:22 and 1:9:27, respectively. These results demonstrate that by controlling the composition of the capping ligands good control over the shape of the resulting nanocrystals can be achieved during the growth process. The selective adsorption of the strongly binding ligand oleic acid on certain crystal faces during the crystal growth results in the formation of nanorods or square plates.

Parts a and b of Figure 6 display the room-temperature UV absorption and the PL spectra of the Tb_2O_3 and Eu_2O_3 nanorods dispersed in dichloromethane, respectively, as representatives of the optical properties of nanorods synthesized in this work. The intense absorption peak observed at 223 nm for Tb_2O_3 (due to the $4f^8 \rightarrow 4f^75d$ transition) is similar to the absorption edge at 225 nm characteristic of the 4 nm Tb_2O_3 nanocrystals.[34] The absence of a peak at 267 nm indicates the absence of the OH^- ions, and the absence of any feature at around 400−600 nm confirms that the absorption is due to the Tb^{3+} ions with no contributions from the Tb^{4+} ions, thus confirming the high purity of the Tb_2O_3 nanorods.[34] The PL spectrum shows the most intense peak at 540 nm (corresponding to the $^5D_4 \rightarrow {}^4F_5$ transition), consistent with the presence of high concentration of the Tb^{3+} ions.[35]

The PL spectrum of the Eu_2O_3 nanorods (Figure 6b) is described by the $^5D_0 \rightarrow {}^7F_{1,2,3,4}$ transitions of the Eu^{3+} ions.[35] Although the positions of the observed lines are similar to those observed for the Eu^{3+}-doped Y_2O_3 nanocrystals[35] and for the bulk polycrystalline cubic Eu_2O_3 powder,[36] the intensity distributions are significantly different. Specifically, the PL of the nanorods is characterized by strong split peaks at 612 and 620 nm that appear as a single broad peak centered around 615 nm in the Eu_2O_3 nanoparticles.[35] The difference is probably due to the different surface sites occupied by the Eu^{3+} ions in the nanorods and nanoparticles. Detailed PL properties of the rare earth nanorods synthesized by MWI are currently under investigation in our laboratory.

In conclusion, we report a simple and rapid synthetic method of uniform, high-quality rare earth oxide nanorods, nanowires, and nanoplates by microwave irradiation. The method is general, applies to a large variety of metal oxides, and provides a scalable and flexible approach for device applications. The highly uniform nature of the rare earth oxide nanostructures and their spontaneous assembly to form superlattice structures coupled

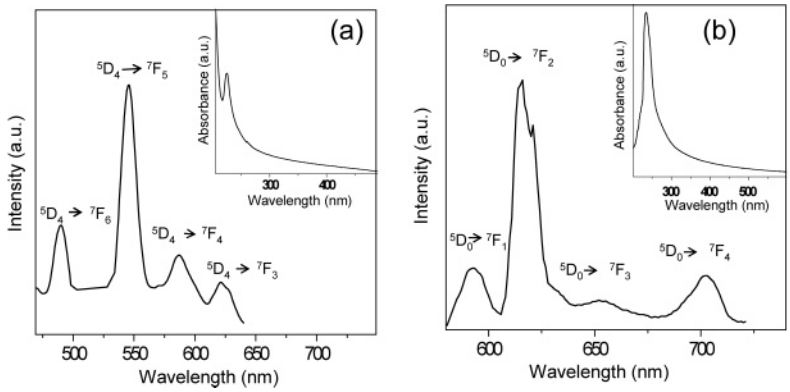

Figure 6. Room-temperature UV−vis absorption (inset) and PL spectra of the nanorods of (a) Tb_2O_3 excited at 300 nm and (b) Eu_2O_3 excited at 270 nm.

with the electronic and optical properties of the 4f electrons are expected to provide a wide range of functional materials for new high-performance luminescence and magnetic devices.

Acknowledgment. We thank the National Science Foundation (CHE-0414613) for support of this work.

References and Notes

(1) (a) Schmid, G. *Nanoparticles from Theory to Application*; Wiley-VCH: Weinheim, Germany, 2004. (b) Ozin, G. A.; Arsenault, A. C. *Nanochemistry*; RSC Publishing: Cambridge, U.K., 2005.

(2) Wang, J. F.; Gudiksen, M. S.; Duan, X. F.; Cui, Y.; Lieber, C. M. *Science* **2001**, *293*, 1455.

(3) Hu, J.; Li, L.; Yang, W.; Manna, L.; Wang, L.; Alivisatos, A. P. *Science* **2001**, *292*, 2060.

(4) Yada, M.; Kitamura, H.; Ichinose, A.; Machida, M.; Kijima, T. *Angew. Chem., Int. Ed.* **1999**, *38*, 3506.

(5) Stouwdam, J. W.; van Veggel, F. C. J. M. *Nano Lett.* **2002**, *2*, 733.

(6) Kompe, K.; Borchert, H.; Storz, J.; Lobo, A.; Adam, S.; Moller, T.; Haase, M. *Angew. Chem., Int. Ed.* **2003**, *42*, 5513.

(7) Meltzer, R. S.; Feofilov, S. P; Tissue, B.; Yuan, H. B. *Phys. Rev. B.* **1999**, *60*, R14012.

(8) *Handbook on the Physics and Chemistry of Rare Earths*; Gschneider, K. A., Jr., Eyring, L., Eds.; North-Holland: New York, 1983.

(9) Kadowakim, Y.; Aika, K. *J. Catal.* **1996**, *161*, 178.

(10) Jiang, Y. D.; Wang, Z. L.; Zhang, F. L.; Paris, H. G.; Summers, C. J. *J. Mater. Res.* **1998**, *13*, 2950.

(11) Li, R.; Yabe, S.; Yamashita, M.; Momose, S.; Yoshida, S.; Yin, S.; Sato, T. *Solid State Ionics* **2002**, *151*, 235.

(12) Flytzani-Stephanopoulos, M.; Sakbodin, M.; Wang, Z. *Science* **2006**, *312*, 1508.

(13) Hsu, W. P.; Nnquist, L. R.; Matijevic, E. *Langmuir* **1988**, *4*, 31.

(14) Wakefield, G.; Keron, H. A.; Dobson, P. J.; Hutchison, *J. Phys. Chem. Solids* **1999**, *60*, 503.

(15) Yada, M.; Mihara, M.; Mouri, S.; Kuroki, M.; Kijima, T. *Adv. Mater.* **2002**, *14*, 309.

(16) Wang, X.; Sun, X. M.; Yu, D. P.; Zou, B. S.; Li, Y. D. *Adv. Mater.* **2003**, *15*, 1442.

(17) Liu, T.; Zhang, Y.; Shao, H.; Li, X. *Langmuir* **2003**, *19*, 7569.

(18) Cao, Y. C. *J. Am. Chem. Soc.* **2004**, *126*, 7456.

(19) Si, R.; Zhang, Y. W.; You, L. P.; Yan, H. Y. *Angew. Chem., Int. Ed.* **2005**, *44*, 3256.

(20) Yu, T.; Joo, J.; Park. Y.; Hyeon, T. *J. Am. Chem. Soc.* **2006**, *128*, 1786.

(21) Wang, X.; Li, Y. D. *Chem.—Eur. J.* **2003**, *9*, 5627.

(22) Patra, C. R.; Alexandra, G.; Patra, S.; Jacob, D. S.; Gedanken, A.; Landau, A.; Gofer, Y. *New J. Chem.* **2005**, *29*, 733.

(23) Wang, X. J.; Gao, M. Y. *J. Mater. Chem.* **2006**, *16*, 1360.

(24) Mai, H. X.; Zhang, Y. W.; Si, R.; Yan, Z. G.; Sun, L. D.; You, L. P.; Yan, C. H. *J. Am. Chem. Soc.* **2006**, *128*, 6426.

(25) He, J.; Zhao, X. N.; Zhu, J. J.; Wang, J. *J. Cryst. Growth* **2002**, *240*, 389.

(26) Murgan, A. V.; Sonawane, R. S.; Kale, B. B.; Apte, S. K.; Kulkarni, A. V. *Mater. Chem. Phys.* **2001**, *71*, 98.

(27) Chen, D.; Tang, K.; Shen, G.; Sheng, J.; Fang, Z.; Liu, X.; Zheng, H.; Qian, Y. *Mater. Chem. Phys.* **2003**, *82*, 206.

(28) Gerbec, J. A.; Magana, D.; Washington, A.; Strouse, G. F. *J. Am. Chem. Soc.* **2005**, *127*, 15791.

(29) Glaspell, G.; Fuoco, L.; El-Shall, M. S. *J. Phys. Chem. B.* **2005**, *109*, 17350.

(30) Panda, A. B.; Glaspell, G.; El-Shall, M. S. *J. Am. Chem. Soc.* **2006**, *128*, 2790.

(31) Lee Penn, R.; Banfield, J. F. *Science* **1998**, *281*, 969.

(32) Puntes, V. F.; Zanchet, D.; Erdonmez, C. K.; Alivisatos, A. P. *J. Am. Chem. Soc.* **2002**, *124*, 12874.

(33) Park, J.; An, K.; Hwang, Y.; Park, J.-G.; Noh, H.-J.; Kim, J.-Y.; Park, J.-H.; Hwang, N.-M.; Hyeon, T. *Nat. Mater.* **2004**, *3*, 891.

(34) Wakefield, G.; Keron, H. A.; Dobson, P. J.; Hutchison, J. L. *J. Phys. Chem. Solids* **1999**, *60*, 503.

(35) Bazzi, R.; Flores-Gonzalez, M. A.; Louis, C.; Lebbou, K.; Dujardin, C.; Brenier, A.; Zhang, W.; Tillement, O.; Bernstein, E.; Perriat, P. *J. Lumin.* **2003**, *102*, 445.

(36) Sheng, K. C.; Korenowski, G. M. *J. Phys. Chem.* **1988**, *92*, 50.